Analysis of Broadside Coupled Strip Inset Dielectric Guide

Z. Fan and S.R. Pennock

School of Electronic and Electrical Engineering
University of Bath, Bath BA2 7AY, U.K.

Abstract

A theoretical and numerical method is presented for the analysis of broadside-coupled strip inset dielectric guide. The method of analysis is based on an integral equation formulation and Galerkin's procedure. In addition to propagation constants for two fundamental and higher order modes, the characteristic impedances for the two fundamental modes are calculated using the total propagating power and the longitudinal strip currents. The propagation characteristics of two fundamental modes are then used to compute 4-port circuit parameters. These are essential for accurate analysis and design of coupled line circuits such as directional couplers.

I. Introduction

The inset dielectric guide (IDG) has been proposed [1] as an alternative to image line. IDG has demonstrated advantages in terms of confinement of the electromagnetic field, low radiation loss at bends, possible ease of fabrication by use of plastic moulding and spray metallization techniques, and inclusion of devices such as diodes with little performance degradation[2]. It has been also shown [3] that the twin layer IDG with high permittivity layer at the top of the groove exhibits very wide monomode bandwidth exceeding that of double ridge waveguide. In addition, the IDG can be integrated with other planar structures such as microstrip line [4]. This can be used for feeding planar antennas or as a low loss transmission line. In the latter case the propagation of surface modes, which can effect the performance of microstrip line, is prevented by the side walls of the groove.

The effective dielectric constant method [5] was first used to the analysis of the IDG structure. The transverse resonance diffraction (TRD) technique was then applied to IDG, and by taking into account the field singular boundary condition at the 90^0 metal edges, accurate results were obtained for the propagation constants of the first few modes and Q factors [1]. The TRD method has also been extended to analyze the propagation characteristics of microstrip loaded IDG, embedded strip IDG and broadside coupled strip IDG structures [4, 6, 7]. Published data for broadside coupled strip IDG are limited to the propagation constants of two fundamental modes only. However, a knowledge of the characteristic impedances is required if circuits, such as couplers, filters and antennas, are to be designed using broadside coupled strip IDG. This paper presents a rigorous method for calculating propagation constants and characteristic impedances of the broadside coupled strip IDG, and hence, the 4-port parameters of its equivalent circuit.

II. Formulation of Integral Equations

Figure 1 shows the cross section of broadside-coupled strip inset dielectric guide and the coordinate system used in the analysis. An $\exp j(\omega t - \beta z)$ time and z dependence is assumed for all field and current quantities. Electromagnetic field components in the slot region can be represented through their discrete Fourier transforms:

$$E_y(x,y) = \frac{1}{a}\sum_{n=-\infty}^{\infty} \tilde{E}_y(\alpha_n, y)e^{-j\alpha_n x} \quad (1)$$

and similarly for other field components. In order to satisfy the electric field boundary conditions at the sidewalls of the slot, the values of α_n are constrained to be $\alpha_n = \frac{2n\pi}{a}$ for the E_z odd modes, $\alpha_n = \frac{(2n+1)\pi}{a}$ for the E_z even modes including two fundamental modes, where $n = 0, \pm1, \pm2, \cdots$.

Since the air region is unbounded in x, field components in the air region are expressed in terms of continuous Fourier transforms, for example:

$$E_y(x,y) = \frac{1}{2\pi}\int_{-\infty}^{\infty} \tilde{E}_y(\alpha, y)e^{-j\alpha x}\, d\alpha \quad (2)$$

Solutions to the wave equations in Fourier transformed domain are obtained for the different regions of the structure (air, upper and lower dielectric layers in the slot). The solutions contain coefficients, which are determined by applying the boundary conditions at infinity, on the base of

BB

CH3277-1/93/0000-0839$01.00 © 1993 IEEE

the slot and across the lower interface and introducing the electric field components transverse to y at the upper interface. Enforcing the conditions that the current density components at $y = 0$ vanish for $\frac{w_1}{2} < |x| < \frac{a}{2}$ and that the tangential electric field components at $y = -h_1$ vanish for $|x| < \frac{w_2}{2}$ leads to four integral equations for tangential electric field components at $y = 0$ and current components at $y = -h_1$.

$$\begin{aligned}
&\frac{1}{2\pi}\int_{-\infty}^{\infty}[Y_{i1}^a \tilde{E}_x^u(\alpha) + Y_{i2}^a \tilde{E}_z^u(\alpha)]e^{-j\alpha x}d\alpha \\
&\quad +\frac{1}{a}\sum_{n=-\infty}^{\infty}[Y_{i1}^s \tilde{E}_x^u(\alpha_n) + Y_{i2}^s \tilde{E}_z^u(\alpha_n) \\
&\qquad +Y_{i3}^s \tilde{J}_x^l(\alpha_n) + Y_{i4}^s \tilde{J}_z^l(\alpha_n)]e^{-j\alpha_n x} \\
&\quad = 0 \quad \text{for} \quad \frac{w_1}{2} < |x| < \frac{a}{2} \quad i = 1,2
\end{aligned} \tag{3}$$

$$\begin{aligned}
&\frac{1}{a}\sum_{n=-\infty}^{\infty}[Y_{i1}^s \tilde{E}_x^u(\alpha_n) + Y_{i2}^s \tilde{E}_z^u(\alpha_n) \\
&\quad +Y_{i3}^s \tilde{J}_x^l(\alpha_n) + Y_{i4}^s \tilde{J}_z^l(\alpha_n)]e^{-j\alpha_n x} \\
&\quad = 0 \quad \text{for} \quad |x| < \frac{w_2}{2} \quad i = 3,4
\end{aligned} \tag{4}$$

where $\tilde{E}_x^u(\alpha_n) = (\int_{-\frac{a}{2}}^{-\frac{w_1}{2}} + \int_{\frac{w_1}{2}}^{\frac{a}{2}})E_x^u(x)e^{j\alpha_n x}dx$

$\tilde{E}_z^u(\alpha_n) = \frac{j}{\alpha_n}(\int_{-\frac{a}{2}}^{-\frac{w_1}{2}} + \int_{\frac{w_1}{2}}^{\frac{a}{2}})\frac{\partial E_z^u(x)}{\partial x}e^{j\alpha_n x}dx$

$\tilde{J}_x^l(\alpha_n) = \frac{j}{\alpha_n}\int_{-\frac{w_2}{2}}^{\frac{w_2}{2}}\frac{\partial J_x^l(x)}{\partial x}e^{j\alpha_n x}dx$

$\tilde{J}_z^l(\alpha_n) = \int_{-\frac{w_2}{2}}^{\frac{w_2}{2}} J_z^l(x)e^{j\alpha_n x}dx$

It is noted that $\frac{\partial E_z^u(x)}{\partial x}$ and $\frac{\partial J_x^l(x)}{\partial x}$ are used instead of $E_z^u(x)$ and $J_x^l(x)$ because they satisfy the same boundary and singular edge conditions as $E_x^u(x)$ and $J_z^l(x)$, respectively. This choice also improves convergence of the solution of the integral equations.

III. Application of Galerkin's Method

In order to solve integral equations (3) - (4), Galerkin's method is applied. Expanding electric field components E_x^u and $\frac{\partial E_z^u}{\partial x}$ and current components $\frac{\partial J_x^l}{\partial x}$ and J_z^l in terms of known basis functions and taking the inner product of the integral equations with basis functions yield a homogeneous matrix equation for the unknown expansion coefficients. Nontrivial solutions may be obtained by requiring the determinant of the coefficient matrix to be zero. This condition results in the determinantal equation for the propagation constant. In order to achieve fast convergence to the solutions of the determinantal equation, the edge conditions satisfied by tangential electric field components on the upper interface and current components on the lower strip should be accounted for in choosing the basis functions. Here, basis functions are chosen to be a complete set of orthonomalized functions weighted by an appropriate singular function which describes the edge conditions. Thus the basis functions E_{xm}^u and $\frac{\partial E_{zm}^u}{\partial x}$ can be chosen as

$$\begin{aligned}
E_{xm}^u(x) &= \frac{\partial E_{zm}^u(x)}{\partial x} = \frac{1}{N_m^P}(1-x')^{-\frac{1}{3}}(1+x')^{-\frac{1}{2}} \\
&\quad \begin{cases} P_m^{(-\frac{1}{3},-\frac{1}{2})}(x') \text{ for } \frac{w_1}{2} < x < \frac{a}{2} \\ \pm P_m^{(-\frac{1}{3},-\frac{1}{2})}(x') \text{ for } -\frac{a}{2} < x < -\frac{w_1}{2} \end{cases}
\end{aligned} \tag{5}$$

where $x' = 2(|x| - x_0)/w_s$, $x_0 = (a + w_1)/4$ and $w_s = (a - w_1)/2$. $P_m^{(-\frac{1}{3},-\frac{1}{2})}$ are Jacobi polynomials, and N_m^P are normalization factors. The plus and minus signs in $\pm$ are chosen for the E_z odd and even modes, respectively. It should be noted that for E_{xm}^u the series starts at 0, but for $\frac{\partial E_{zm}^u}{\partial x}$ the series starts at 1.

The basis functions $\frac{\partial J_{xm}^l}{\partial x}$ and J_{zm}^l are chosen as follows

$$\begin{aligned}
\frac{\partial J_{xm}^l(x)}{\partial x} &= J_{zm}^l(x) \\
&= \frac{1}{N_n^T}\left[1-(\frac{2x}{w_2})^2\right]^{-\frac{1}{2}} T_n(\frac{2x}{w_2}) \text{ for } |x| < \frac{w_2}{2}
\end{aligned} \tag{6}$$

where T_n are Chebyshev polynomials, and N_n^T are normalization factors. $n = 2m+1$ and $n = 2m$ are chosen for the E_z odd and even modes, respectively. Note that $m = 0, 1, 2\ldots$ except that $m = 1, 2, \ldots$ for $\frac{\partial J_{xm}^l}{\partial x}$ for the E_z even mode.

IV. Characteristic Impedances

The existence of two conducting strips in the IDG structure implies that two fundamental modes without cut-off frequencies can be supported by the structure. Once the propagation constants of two fundamental modes, β_1 and β_2 are found, the total power flow P_j along the guide for each mode and total longitudinal currents I_{ij} on each conducting strip for each mode can be evaluated, where i=1 for the lower strip, 2 for the upper strip and j=1 for mode 1, 2 for mode 2. The circuit voltage V_{ij} at strip i due to mode j can be found by using the definition of modal power and the reciprocity theorem [8].

$$P_j = \frac{1}{2}\int_s \vec{E}_j \times \vec{H}_j^* \cdot d\vec{s} = \frac{1}{2}\sum_{k=1}^{2} V_{kj}I_{kj}^* \quad (j = 1,2) \tag{7}$$

$$\frac{1}{2}\int_s \vec{E}_i \times \vec{H}_j \cdot ds = \frac{1}{2}\sum_{k=1}^{2} V_{ki}I_{kj} = 0 \; (i,j = 1,2; i \neq j) \tag{8}$$

A characteristic impedance Z_{ij} of strip i for mode j is defined as

$$Z_{ij} = \frac{V_{ij}}{I_{ij}} \tag{9}$$

V. Numerical Results

It has been found from numerical results that two or three basis functions for each expansion quantity are sufficient to obtain accurate solutions for propagation constants to four significant digits, but more basis functions are required for accurate solutions for the characteristic impedances. Numerical computations also show that two fundamental modes without cutoff frequencies are the first two E_z even modes.

Comparison of the present results with calculated and measured results available in [7] is shown in Figure 2 for the propagation constants of the two fundamental modes. Clearly the agreement between these data is good.

Figure 3 shows the equivalent coupled-line circuit for the broadside coupled strip IDG. Once propagation constants, characteristic impedances and strip current ratios of two fundamental modes are found, 4-port circuit parameters of the equivalent circuit can be calculated using the expressions in [9]. Results of the S parameters S_{11}, S_{21}, S_{31} and S_{41} as a function of frequency are presented in Figure 4. It is observed that the maximum coupling (S_{31}) from port 1 to port 3 is obtained when $(\beta_1 + \beta_2)l = \pi$ at 4 GHz.

Figure 5 shows S parameters as a function of the width of the upper strip. It can be observed that S_{41} is the most greatly affected by the change of w_1. There exists a minimum value of S_{41} at a certain value of w_1. Figure 6 shows S parameters as a function of the width of the lower strip. It can be seen that S_{11} and S_{41} are greatly affected by the change of w_2. There exist minimum values for the curves of S_{11} and S_{41}, respectively. Figure 7 shows S parameters as a function of the thickness of the upper substrate. It can be found that S_{31} (the coupling from port 1 to port 3) increases as h_1 decreases. From Figure 5 to 7, it is concluded that weak and strong directional couplers with good input match and high isolation can be realized by the change of the value of h_1 and appropriate choices of values of w_1 and w_2. In these couplers, the coupling occurs in the backward direction.

VI. Conclusion

This paper presents a theoretical and numerical method for calculating propagation constants and characteristic impedances of broadside coupled strip IDG by means of integral equation formulation and Galerkin's method. 4-port circuit parameters such as scattering matrix are also calculated in terms of propagation characteristics of two fundamental modes. Numerical results for scattering parameters are presented for various values of structural parameters. It is found that both weak and strong directional couplers can be realized by using a section of this structure with appropriate choices of the distance between the strips and the widths of the strips.

References

[1] T. Rozzi and S. J. Hedges, "Rigorous analysis and network modeling of the inset dielectric guide", IEEE Trans. Microwave Theory Tech., Vol.MTT-35, pp.823-833, Sept. 1987.

[2] S.R. Pennock, T. Rozzi & A. DiFilippo, "Inset dielectric guide mounting of a detector diode", IEEE Microwave and Guided Wave Letters, Vol 1, pp.168-170, May 1992

[3] S. R. Pennock, N. Izzat and T. Rozzi, "Very wideband operation of twin-layer inset dielectric guide", IEEE Trans. Microwave Theory Tech., Vol.MTT-40, pp.1910-1917, Oct. 1992.

[4] T. Rozzi, A. Morini and G. Gerini, "Analysis and applications of microstrip loaded inset dielectric waveguide", IEEE Trans. Microwave Theory Tech., Vol.MTT-40, pp.272-278, Feb. 1992.

[5] W. Zhou and T. Itoh, "Analysis of trapped image guides using effective dielectric constant and surface impedances", IEEE Trans. Microwave Theory Tech., Vol.MTT-30, pp.2163-2166, Dec. 1982.

[6] T. Rozzi, G. Gerini, A. Morini and M. Santis, "Multilayer buried microstrip inset guide", in Proc. 21th European Microwave Conf., Stultgart pp.673-678, 1991

[7] N. Izzat. "Space domain analysis of inhomogeneous waveguides of the microstrip and inset guide families", Ph.D Thesis, Bath University, Bath, 1991.

[8] F. L. Mesa, G. Cano, F. Medina, R. Marques and M. Horno, "On the quasi TEM and full wave approaches applied to coplanar multistrip on lossy dielectric layered media", IEEE Trans. Microwave Theory Tech., Vol.MTT-40, pp.524-532, March 1992.

[9] V. K. Tripathi, "Asymmetric coupled transmission lines in an inhomogeneous medium", IEEE Trans. Microwave Theory Tech., Vol.MTT-23, pp.734-739, 1975.

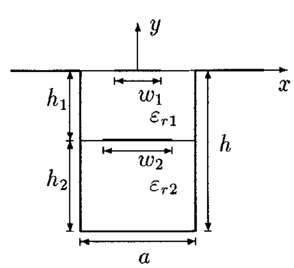

Figure 1: Cross section of a broadside coupled strip inset dielectric guide and the coordinate system used in the analysis

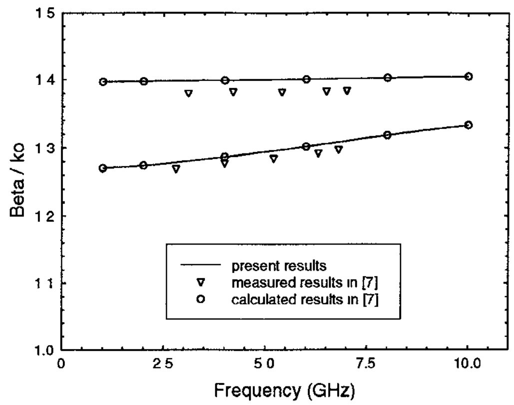

Figure 2: Dispersion characteristics of two fundamental modes (a =2.286e–2 m, h_1 =2.16e–3 m, h_2 =8.0e–3 m, ε_{r1} = 2.04, ε_{r2} = 2.04, w_1 =5.0e–3 m and w_2 =1.0e–2 m)

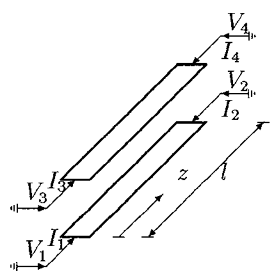

Figure 3: Equivalent circuit for broadside coupled strip IDG

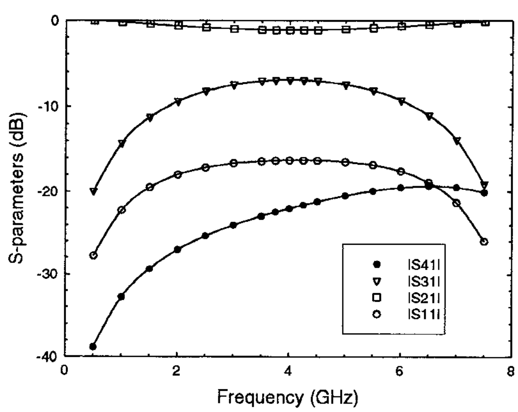

Figure 4: S parameters as a function of frequency (a =1.016e–2 m, h_1 =2.54e–3 m, h_2 =1.27e–2 m, ε_{r1} = 2.04, ε_{r2} = 2.04, w_1 =7.0e–3 m, w_2 =5.0e–3 m, Z_0 = 50 Ω and l =1.39e–2 m)

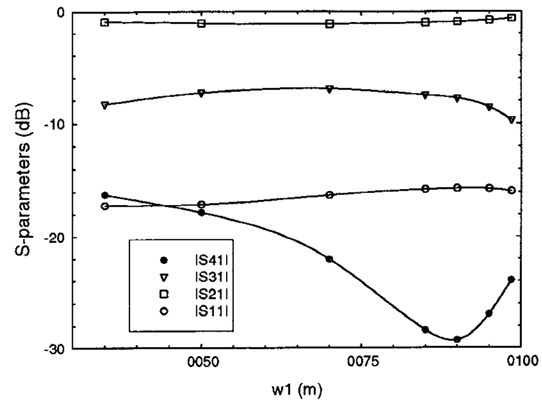

Figure 5: S parameters as a function of w_1 (a =1.016e–2 m, h_1 =2.54e–3 m, h_2 =1.27e–2 m, ε_{r1} = 2.04, ε_{r2} = 2.04, w_2 =5.0e–3 m, f =4 GHz, Z_0 = 50 Ω and $l = \pi/(\beta_1+\beta_2)$)

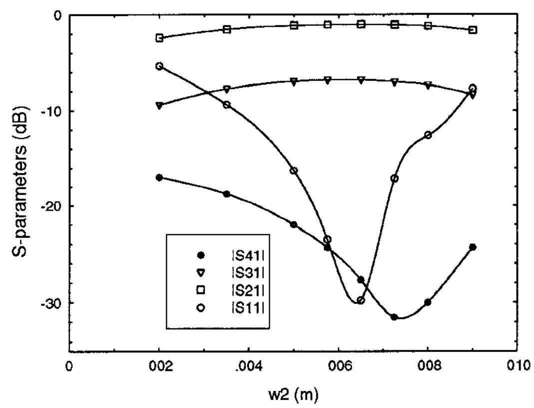

Figure 6: S parameters as a function of w_2 (a =1.016e–2 m, h_1 =2.54e–3 m, h_2 =1.27e–2 m, ε_{r1} = 2.04, ε_{r2} = 2.04, w_1 =7.0e–3 m, f =4 GHz, Z_0 = 50 Ω and $l = \pi/(\beta_1+\beta_2)$)

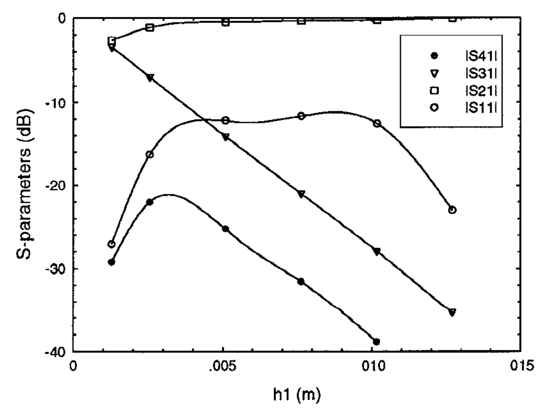

Figure 7: S parameters as a function of h_1 (a =1.016e–2 m, h =1.524e–2 m, ε_{r1} = 2.04, ε_{r2} = 2.04, w_1 =7.e–3 m, w_2 =5.0e–3 m, f =4 GHz, Z_0 = 50 Ω and $l = \pi/(\beta_1+\beta_2)$)